



Environmentally weathered polystyrene particles induce phenotypical and functional maturation of human monocyte-derived dendritic cells

Annemijne E. T. van den Berg, Maud Plantinga, Dick Vethaak, Kas J. Adriaans, Marianne Bol-Schoenmakers, Juliette Legler, Joost J. Smit & Raymond H. H. Pieters

To cite this article: Annemijne E. T. van den Berg, Maud Plantinga, Dick Vethaak, Kas J. Adriaans, Marianne Bol-Schoenmakers, Juliette Legler, Joost J. Smit & Raymond H. H. Pieters (2022) Environmentally weathered polystyrene particles induce phenotypical and functional maturation of human monocyte-derived dendritic cells, *Journal of Immunotoxicology*, 19:1, 125-133, DOI: [10.1080/1547691X.2022.2143968](https://doi.org/10.1080/1547691X.2022.2143968)

To link to this article: <https://doi.org/10.1080/1547691X.2022.2143968>



© 2022 The Author(s). Published by Informa UK Limited, trading as Taylor & Francis Group.



Published online: 24 Nov 2022.



[Submit your article to this journal](#)



Article views: 110



[View related articles](#)









[View Crossmark data](#)

RESEARCH ARTICLE



Environmentally weathered polystyrene particles induce phenotypical and functional maturation of human monocyte-derived dendritic cells

Annemijne E. T. van den Berg^a , Maud Plantinga^b , Dick Vethaak^{a,c} , Kas J. Adriaans^a ,
Marianne Bol-Schoenmakers^a , Juliette Legler^a , Joost J. Smit^a  and Raymond H. H. Pieters^a 

^aInstitute for Risk Assessment Sciences, Utrecht University, Utrecht, The Netherlands; ^bCenter for Translational Immunology, University Medical Centre Utrecht, Utrecht, The Netherlands; ^cDepartment of Environment and Health, Vrije Universiteit, Amsterdam, The Netherlands

ABSTRACT

Micro- and nanoplastics (MNP) are ubiquitously present in the environment due to their high persistence and bioaccumulative properties. Humans get exposed to MNP via various routes and consequently, they will encounter dendritic cells (DC) which are antigen-presenting cells involved in regulating immune responses. The consequences of DC exposure to MNP are an important, yet understudied, cause of concern. Therefore, this study aimed to assess the uptake and effect of MNP *in vitro* by exposing human monocyte-derived dendritic cells (MoDC) to virgin and environmentally weathered polystyrene (PS) particles of different sizes (0.2, 1, and 10 µm), at different concentrations ranging from 1 to 100 µg/ml. The effects of these particles were examined by measuring co-stimulatory surface marker (i.e. CD83 and CD86) expression. In addition, T-cell proliferation was measured via a mixed-leukocyte reaction (MLR) assay. The results showed that MoDC were capable of absorbing PS particles, and this was facilitated by pre-incubation in heat-inactivated (HI) plasma. Furthermore, depending on their size, weathered PS particles in particular caused increased expression of CD83 and CD86 on MoDC. Lastly, weathered 0.2 µm PS particles were able to functionally activate MoDC, leading to an increase in T-cell activation. These *in vitro* data suggest that, depending on their size, weathered PS particles might act as an immunostimulating adjuvant, possibly leading to T-cell sensitization.

ARTICLE HISTORY

Received 15 September 2022
Revised 27 October 2022
Accepted 1 November 2022

KEYWORDS

Micro- and nanoplastics; immunotoxicology; polystyrene; adjuvant effect; immune sensitization

Introduction

Micro- and nanoplastics (MNP) have increasingly polluted the environment and are amassing in virtually all ecosystems due to their high persistence and bioaccumulative properties (Barboza et al. 2018; SAPEA 2019). MNP are generally defined as plastic particles smaller than 5 mm (microplastics [MP]) and smaller than 1 µm (nanoplastics [NP]) (WHO 2022). They can be divided into primary MNP, which are intentionally produced for industrial applications or products, such as cosmetics, and secondary MNP, which result from environmental degradation of large plastic objects via processes, such as UV light exposure and physical abrasion (EFSA 2016). Most secondary MNP originate from plastic packages, drinking bottles, synthetic textiles, fishing gear, and car tires (Barboza et al. 2018). Major synthetic polymers that make up MNP include polystyrene (PS), polyethylene (PE), polypropylene (PP), and polyamide (PA). MNP are highly heterogeneous in size, shape, and chemical composition. These divergent characteristics can influence their aging, fate, and toxicity (Hidalgo-Ruz et al. 2012; Andraday 2017; Vethaak and Legler 2021).

Due to their small size, MNP are easily spread throughout the environment and undoubtedly, humans get exposed to MNP via various exposure routes, in particular via inhalation and ingestion (Carbery et al. 2018). Several studies have tried to estimate the average amount of MNP ingested by humans through various pathways (Cox et al. 2019; Senathirajah et al. 2021).

However, exposure data is often based on non-standardized, preliminary results, and even misperceptions and thus specific knowledge on human exposure to MNP is still limited (Koelmans et al. 2017; Vethaak and Legler 2021). Multiple *in vitro* and *in vivo* studies show that MNP accumulate in the intestines of various species and can cross the intestinal barrier and consequently reach systemic circulation (Hirt and Body-Malapel 2020; Prata et al. 2020). Recently, a Dutch study found a mean sum concentration of 1.6 µg/ml of total polymers in blood samples of healthy donors, supporting the hypothesis of absorption of MNP into the bloodstream (Leslie et al. 2022). This finding illustrates that MNP cross epithelial linings and enters the systemic blood circulation. Though the extent of MNP crossing over epithelial linings is not yet well established, it is imperative to understand their potential systemic immunotoxicological effects (Vethaak and Legler 2021).

Importantly, MNP are known to absorb all sorts of biomolecules and natural organic matter. The resulting outer layer alters the surface properties of the MNP by affecting morphology, charge, and chemistry (Witzmann et al. 2022). This phenomenon may play a crucial role in the interaction of MNP with biological systems and influence the distribution of MNP across cells and retention in tissues (Saptarshi et al. 2013; Schöttler et al. 2016; Ke et al. 2017; Gruber et al. 2020). For instance, once in the blood, MNP may immediately bind plasma proteins, forming a

CONTACT Annemijne E. T. van den Berg  a.e.t.vandenberg@uu.nl  Institute for Risk Assessment Sciences, Utrecht University, Utrecht, The Netherlands

© 2022 The Author(s). Published by Informa UK Limited, trading as Taylor & Francis Group.
This is an Open Access article distributed under the terms of the Creative Commons Attribution License (<http://creativecommons.org/licenses/by/4.0/>), which permits unrestricted use, distribution, and reproduction in any medium, provided the original work is properly cited.

complex protein biofilm (Tenzer et al. 2013). Conceivably, this possibly impacts MNP toxicity.

To date, most studies regarding MNP have been conducted with pristine particles. However, MNP in the environment are subjected to some degree of weathering, leading to possible physical, chemical, and microbial alterations. These environmentally weathered particles may for instance absorb microbial biomolecules. In the intestinal tissue (e.g. lamina propria and draining lymph nodes) and upon systemic circulation, MNP can potentially dysregulate immune responses (Hirt and Body-Malapel 2020; Weber et al. 2022). Research has shown that the addition of for instance lipopolysaccharide (LPS) to innocuous gold nanoparticles leads to a synergistic increase in the release of pro-inflammatory cytokines, such as interleukin (IL)-1 β and tumor necrosis factor (TNF)- α (Boyles et al. 2015; Li et al. 2017). For the same reason, exposure to environmentally weathered MNP might result in increased inflammatory responses (Noventa et al. 2021).

Professional antigen-presenting dendritic cells (DC) are critical for initiating adaptive immune responses. They occur in relatively high frequency in the intestines and are constantly interacting with antigens from the lumen of the gut. DC are involved in instructing whether a tolerance-inducing or sensitizing response occurs toward a particular antigen (Coomes and Powrie 2008). Upon maturation, co-stimulatory molecules (like CD83 and CD86) are up-regulated, so the DC can enhance effector responses by releasing cytokines and activating naïve T-cells (Seydoux et al. 2014; Stagg 2018). Given the critical role of DC in managing adaptive immune responses, the effect of MNP exposure on DC maturation is important to ascertain.

To date, a limited number of studies have demonstrated the uptake of PS particles by DC (Foged et al. 2005; Rothen-Rutishauser et al. 2007; Weber et al. 2022) and the maturation of MNP-exposed DC is still largely understudied (Frick et al. 2012; Mathaes et al. 2015). In addition, the majority of toxicity studies have used virgin, manufactured particles that may not be representative of real environmental exposure. Therefore, this study aimed to assess the uptake and effects of MNP *in vitro* by exposing human monocyte-derived DC (MoDC) to virgin and environmentally-weathered PS particles of different sizes (0.2, 1, and 10 μ m). To investigate the effect of a plasma protein biofilm, the particles were pre-incubated in heat-inactivated (HI) plasma. The effect of virgin and weathered PS particles was examined with a focus on the phenotypical and functional maturation of human MoDC. This was accomplished by measuring co-stimulatory surface markers (i.e. CD83 and CD86). Furthermore, T-cell activation by MoDC was measured via a mixed leukocyte reaction (MLR) assay.

Materials and methods

Human MoDC isolation

EDTA-treated whole blood (WB) was collected from an in-house healthy donor service at the University Medical Center Utrecht (UMCU), the Netherlands. All blood donors provided written consent before participating in the in-house donor service. Participant information was kept confidential.

The isolation of peripheral blood mononuclear cells (PBMC) was executed within 4 h by standard density centrifugation using a Ficoll-Paque PLUS gradient (GE Healthcare Bio-Sciences AB, Chicago, IL). During the isolation process, plasma was removed from the gradient and was stored at -20°C until later use for

heat inactivation and pre-incubation with the PS particles. Next, monocytes were isolated from the fresh PBMC using a Percoll gradient (GE Healthcare Bio-Science, Piscataway, NJ). The monocytes were then incubated in T25 culture flasks in a 37°C and 5% CO_2 atmosphere (at density of $1.5\text{--}3.0 \times 10^6$ cells/ml) in 6 ml of RPMI 1640 medium supplemented with 10% heat-inactivated fetal calf serum (HI-FCS) and 1% penicillin/streptomycin (all products from Gibco, Waltham, MA). For differentiation into MoDC, human GM-CSF (75 ng/ml), and human IL-4 (25 ng/ml) (Miltenyi Biotec, Bergisch Gladbach, Germany) were added for 6 d. After differentiation, MoDC were collected and plated into 96-well flat bottom plates at a density of 2.0×10^5 cells/well in 100 μ l supplemented RPMI (Greiner, Alphen aan den Rijn, the Netherlands). Plates were then incubated for 1 h at 37°C and 5% CO_2 and directly used for the experiments. MoDC and plasma from one donor were used for each independent experiment.

Particle preparation

Non-functionalized Fluoresbrite Yellow Green PS particles were purchased in three different sizes; 0.2, 1, and 10 μ m (Polysciences, Inc., Warrington, PA). These PS particles are internally-dyed with fluorescein and packaged as 2.5% aqueous suspensions. In addition, virgin and weathered non-fluorescent PS particles were used that were kindly gifted by Deltares (Delft, the Netherlands). The particles were weathered in glass bottles filled with river water (location = Tolakkerlaan [approximate coordinates $52^{\circ}04'58.4''\text{N}$ $5^{\circ}11'37.1''\text{E}$], Utrecht, the Netherlands). Samples were collected in pre-sterilized 1 L glass bottles, which were opened 1–20 cm below the water surface and filled with water, then filtered through a standard paper filter. Next, the weathering was performed in a duplicate set-up, in glass bottles for 4 weeks at room temperature with exposure to sunlight and constant shaking (100 rpm), with a ratio of particles to water of 0.1% (w/v). After weathering, the particles were washed with phosphate-buffered saline (PBS, pH 7.4), separated from the liquid by decanting, pooled, and re-suspended in PBS (at 1% solids [w/v]).

For specific experiments, PS particles were pre-incubated in HI plasma from the same donor as from whom the MoDC were isolated. Here, 10 μ l of PS particle suspension (at 10 mg/ml) was incubated with 10 μ l supplemented RPMI or HI plasma for 2 h at 37°C under constant shaking (at 100 rpm). The plasma was HI by heating it for 30 min in a waterbath at 56°C to inactivate serum complement. Stock solutions of the particles were then diluted in cell-culture medium to obtain the desired concentrations just prior to the experiments.

Exposure dosimetry

Human MoDC were exposed to a mass-based concentration ($\mu\text{g}/\text{ml}$) of PS particles. The PS particle concentrations used in the experiments ranged from 1 to 100 $\mu\text{g}/\text{ml}$. This range is chosen as a proof-of-principle for hazard identification, since specific data on human exposure is limited. The concentrations were also translated to numerical dose (particles/ml) and surface area ($\mu\text{m}^2/\text{ml}$) to enable comparison with literature data (Table 1). Estimations were based on the formula:

$$\text{Number of particles per ml} = \frac{6W \cdot 10^{12}}{\rho \cdot \pi \cdot \varphi^3}$$

Table 1. Different dose metrics for the polystyrene particles used in this study.

Particle size (μm)	Mass-based ($\mu\text{g/ml}$)	Numerical (particles/ml)	Surface area ($\mu\text{m}^2/\text{ml}$)
0.2	1	2.27×10^8	3.46×10^7
	10	2.27×10^9	3.46×10^8
	75	1.70×10^{10}	2.60×10^9
	100	2.27×10^{10}	3.46×10^9
1	1	1.82×10^6	5.71×10^6
	10	1.82×10^7	5.71×10^7
	75	1.35×10^8	4.28×10^8
	100	1.82×10^8	5.71×10^8
10	1	1.71×10^3	5.60×10^5
	10	1.71×10^4	5.60×10^6
	75	1.28×10^5	4.20×10^7
	100	1.71×10^5	5.60×10^7

where W =grams of particles per ml, ρ =density of polymer [in grams/ml; 1.05 for PS], and φ =particle diameter [in micron].

Analysis of particle uptake by flow cytometry

Cells were incubated with 200 μl of 0.2, 1, or 10 μm fluorescent PS particles (with or without HI-plasma pre-treatment) at a concentration of 75 $\mu\text{g/ml}$ for 1 h at 37 °C. After exposure, cells were collected using 50 μl 2 mM EDTA/PBS and washed three times with 200 μl cold PBS to remove PS particles that were not taken up. Next, the cells were incubated with 50 μl F_c Receptor Binding Inhibitor (1:100, Invitrogen, Waltham, MA) for 20 min at 4 °C. After that, they were stained with 50 μl allophycocyanin (APC)-conjugated mouse anti-human CD11c (1:100 dilution; Clone 3.9, Invitrogen) for 30 min at 4 °C. The cells were then resuspended in 100 μl FACS buffer (FB; PBS containing 1% bovine serum albumin [BSA] and 0.1% NaN₃). The amount of particle uptake was then analyzed using a BD AccuriTM C6 flow cytometer (FCM) and BD sampler software (BD Biosciences, Franklin Lakes, NJ). MoDC were gated using the forward and sideward scatter. Within this cell population, an additional step was conducted to distinguish MoDC from normal monocytes by selecting CD11c⁺ cells. Next, the percentage of positive cells, i.e. the percentage of cells that took up one or more PS particles, was determined by measuring the fluorescence per cell. Mean Fluorescent Intensity could not be used as a parameter since the data distribution was bi- and multimodal. Furthermore, non-fluorescent virgin and weathered 10 μm particles were added to DC with and without (HI) plasma pre-incubation in the same manner as previously described. Due to the lack of fluorescence, the percentage of positive cells was determined based on differences in the forward and sideward scatter. In each case, a total of at least 200,000 events were acquired per sample.

Cellular imaging of MNP uptake

For the visualization of MNP internalization by the cells, human MoDC were exposed for 1 h to 200 μl of 0.2, 1, or 10 μm fluorescent PS particles (75 $\mu\text{g/ml}$) that had been pre-incubated with HI plasma (1 h, 37 °C). After exposure, 20 μl from each well was combined with 100 μl FB and plated onto a coverslip using a cytospin centrifuge. After 10 min of air drying, the cells were fixed in 50 μl 2% paraformaldehyde (30 min), washed with PBS, and treated for 30 min with 70 μl permeabilization buffer (2% BSA and 0.1% Triton X-100 in PBS) containing DAPI (1.4 μM) and Alexa FluorTM 568 Phalloidin (1 μM) (both Invitrogen) to stain nuclei and β -actin, respectively. After staining, the cells were washed with PBS and mounted onto slides using Prolong Diamond (Life Technologies, Bleiswijk, the Netherlands). Cells

were then imaged using a Stochastic Optical Reconstruction Microscope (STORM: Nikon Instruments Inc., Amstelveen, the Netherlands).

Analysis of particle effect on inflammatory surface markers

Non-fluorescent virgin and weathered PS particles were pre-incubated in HI plasma and were added to human MoDC at concentrations from 1 to 100 $\mu\text{g/ml}$ and the cells were cultured for 24 h. LPS (Type O111:B4 from *Escherichia coli*; 500 ng/ml, Sigma-Aldrich, Zwijndrecht, the Netherlands) treatment of cells was used as a positive control. After the incubation, the cells were collected and incubated with LIVE/DEADTM-APC stain (1:1000 in PBS, Life Technologies) for 20 min at 4 °C. After that, human F_c Receptor Binding Inhibitor was added and the cells held for a further 20 min at 4 °C. To stain the surface markers, cells were incubated with anti-human fluorescein isothiocyanate (FITC)-conjugated mouse anti-human CD83 (1:100 dilution; Clone HB15e, Invitrogen) and phycoerythrin (PE)-conjugated mouse anti-human CD86- (1:100 dilution; Clone T2.2, Invitrogen) for 30 min at 4 °C. The cells were then resuspended in FACS buffer and CD83 and CD86 expressions were measured on the surface of live-gated human MoDC by flow cytometry (see above for analysis specifics). In addition, the percentage viable MoDC within the sample population was measured using the LIVE/DEADTM-APC stain.

Analysis of particle effects on T-cell activation using a MLR assay

Functional maturation of DC is commonly measured via an MLR assay, as it determines the ability of the DC to activate T-cells (Tourkova et al. 2001). For the MLR assay here, allogeneic T-cells (10⁶ cells/ml) were labeled with cell trace violet (5 μM ; Invitrogen) and co-cultured with MoDC (2 \times 10⁵ cells/ml) in 96-well round-bottom plates (Corning, Corning, NY) at a stimulator:responder ratio of 1:5. Unstimulated cell trace violet-labeled cells served as a negative control. After 4 d, the cells were stained with PerCPCy5.5-conjugated anti-CD8 and PE-conjugated anti-CD4 (at 1:1000 and 1:100 dilutions, respectively: both from BD Bioscience) antibodies and analyzed in the FACS Canto II system. The T-cell proliferation analysis was performed using a proliferation tool in the Flowjo software (Becton Dickinson, Franklin Lakes, NJ) providing the division index, which is the average number of cell divisions that a cell in the original population has undergone.

Data analysis

CD4 and CD8 T-cell division data are shown as means \pm SD, with $n=9$. The rest of the data are presented as individual values. Statistical significance was determined by one- or two-way analysis of variance (ANOVA) with Dunnett's *post-hoc* test. A p value < 0.05 was taken as statistically significant. All data were analyzed using Prism software version 8.3 (GraphPad, San Diego, CA).

Results

PS particles are taken up by human MoDC

The cellular uptake of MNP by human MoDC was assessed by flow cytometry after 1 h of incubation with fluorescent PS particles of various sizes pre-incubated with PBS or HI plasma. Uptake was quantified by measuring the percentage of positive cells. Figure 1(A) displays the gating strategy applied to determine the uptake.

Figure 1(B) shows histograms of the FITC fluorescence measured in cells exposed to the various exposure groups. The resulting percentage of positive cells is displayed in Figure 1(C). These findings show that 0.2 and 1 μm PS particles caused a significant increase in positive cells regardless of pre-incubation with HI plasma. The mean fluorescence intensity could not be used due to the abnormal cell distribution. However, the histograms in Figure 1(B) show that some of the cells exposed to the HI plasma pre-incubated 0.2 μm PS particles are more fluorescent than those exposed to the regular 0.2 μm PS particles. Uptake of

1 μm PS particles was reduced when the particles were pre-incubated in HI plasma. Concerning the 10 μm PS particles, only those pre-incubated with HI plasma caused a significant increase in positive cells.

A similar experiment was conducted with virgin and weathered PS particles, with or without pre-incubation with HI plasma (Figure 2). Since these particles are non-fluorescent, their presence inside the cell was measured by plotting the sideward scatter against the forward scatter, as shown in the gating strategy (Figure 2(A)). Due to visualization limitations of the smaller particles, only 10 μm PS particles were suitable for this assay as they could visually change the sideward scatter of the cells. Results show that for both virgin and weathered PS particles a significant increase in positive cells was found for the 10 μm PS particles pre-incubated in HI plasma compared to non-pre-incubated PS particles (Figure 2(B,C)).

STORM was used to verify that the fluorescent PS particles were taken up inside the cells and not adhering to the outside of the cells (Figure 3). Intracellular particle uptake by MoDC was detected for all three PS particle sizes. The MoDC were capable of taking up multiple 0.2 and 1 μm PS particles per cell and the particles seemed to cluster close to the nucleus. The uptake of the 10 μm PS particles was limited to one particle per cell.

Weathered PS particles increase expression of inflammatory surface markers on MoDC

MoDC were incubated with virgin and weathered PS particles (with and without pre-incubation in HI plasma). The percentage

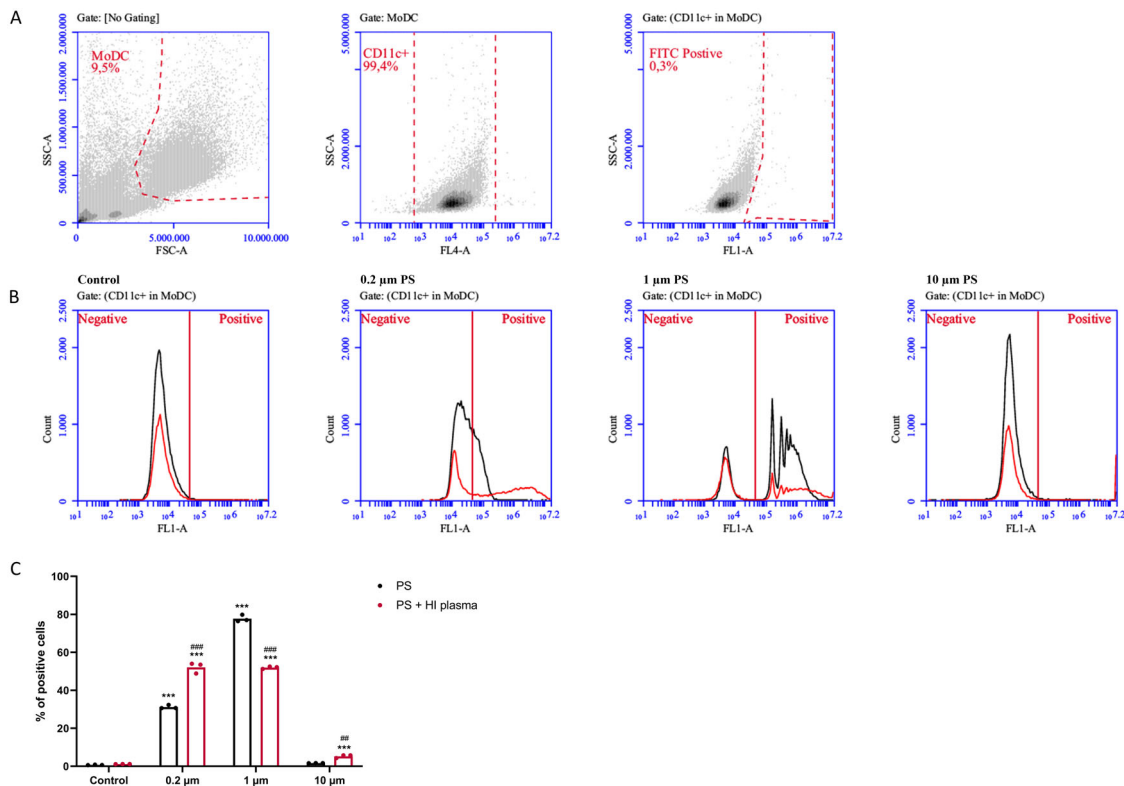


Figure 1. PS particles are taken up by human (monocyte-derived) dendritic cells (MoDC). Cells were exposed for 1 h to YG fluorescent polystyrene (PS) particles (75 $\mu\text{g}/\text{ml}$) which were pre-incubated for 1 h at 37 $^{\circ}\text{C}$ with PBS or heat-inactivated plasma (HI plasma). (A) Gating strategy on flow cytometry plots is shown for control. Left panel shows the initially chosen gate, the middle panel indicates refinement of the gate by selecting cells positive for CD11c staining, and the right panel shows the measured FITC levels in a negative control sample. (B) Histograms of the FITC fluorescence intensity for the different exposure groups. (C) Uptake is expressed by the percentage of positive cells. *** $p < 0.001$, ** $p < 0.01$, and * $p < 0.05$ compared to control. ### $p < 0.001$, ## $p < 0.01$, and # $p < 0.05$ compared to PS without HI plasma pre-incubation.

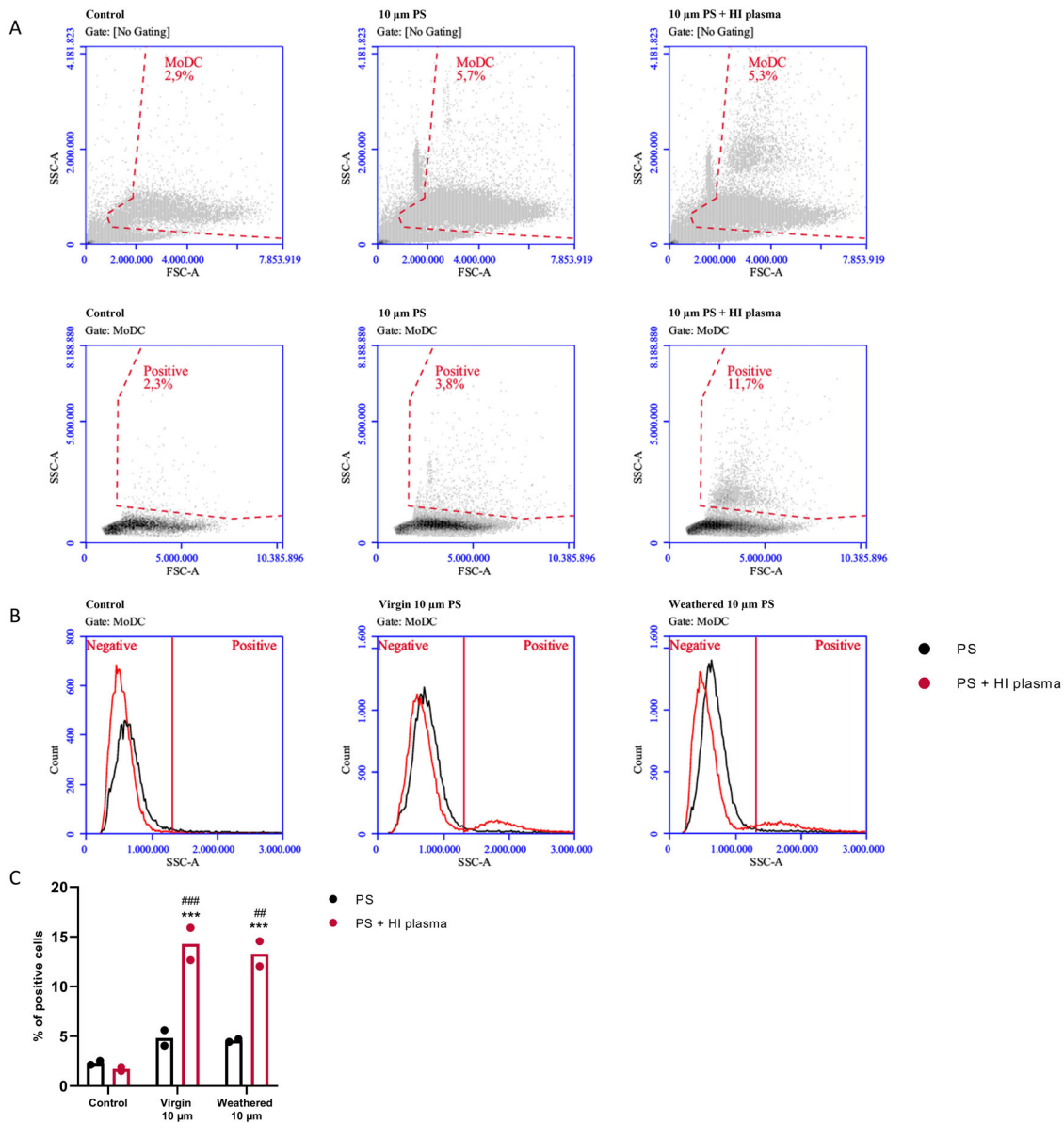


Figure 2. Non-fluorescent virgin and weathered 10 μm PS microplastics are taken up by human DC when pre-incubated in heat-inactivated plasma. Human (monocyte-derived) dendritic cells (MoDC) were exposed to non-fluorescent virgin or weathered 10 μm polystyrene (PS) particles (75 μg/ml) for 2 h. PS particles were pre-incubated with PBS or heat-inactivated plasma (HI plasma) for 1 h at 37 °C. (A) Gating strategy on flow cytometry plots is shown for control, cells exposed to virgin particles and virgin particles + HI plasma. The forward scatter (FSC) and sideward scatter (SSC) were used to gate the dendritic cells (upper panels) and within this gate, the positive cells were selected (lower panels). (B) Histograms are shown of the SSC for the different exposure groups. (C) Uptake is expressed by the percentage of positive cells. ****p* < 0.001 and ***p* < 0.01 compared to control; #*p* < 0.05 compared to PS without HI plasma pre-incubation.

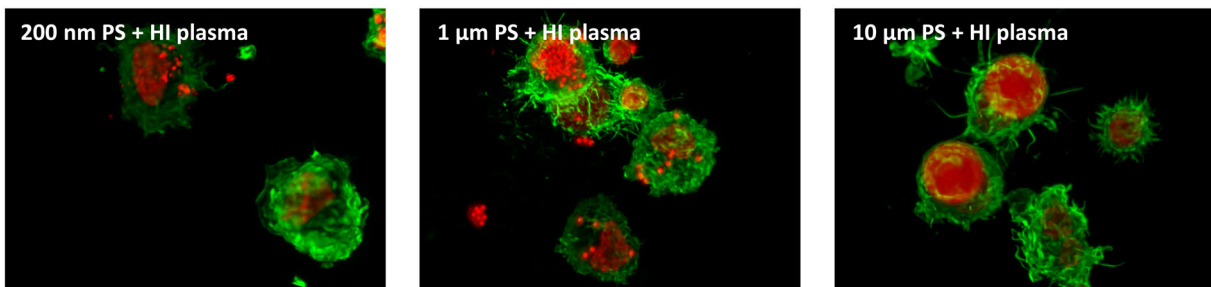


Figure 3. PS micro- and nanoparticles are taken up by human DC as confirmed by microscopy. Human (monocyte-derived) dendritic cells were exposed to fluorescent PS particles (75 μg/ml) for 1 h. PS particles were pre-incubated with heat-inactivated plasma (HI plasma; 1 h, 37 °C). Uptake of 0.2, 1, and 10 μm PS particles was visualized in a Stochastic Optical Reconstruction Microscope (STORM). PS particles are in bright red, nuclei in dark red, and β-actin in green.

of viable MoDC exposed to test concentrations of PS particles was found 90% or higher. To investigate phenotypical DC maturation, two specific co-stimulatory markers (i.e. CD83 and

CD86), typically up-regulated in mature DC, were measured by flow cytometry. Figure 4(A) shows histograms of the fluorescence intensity of CD83 and CD86 staining on the membrane of

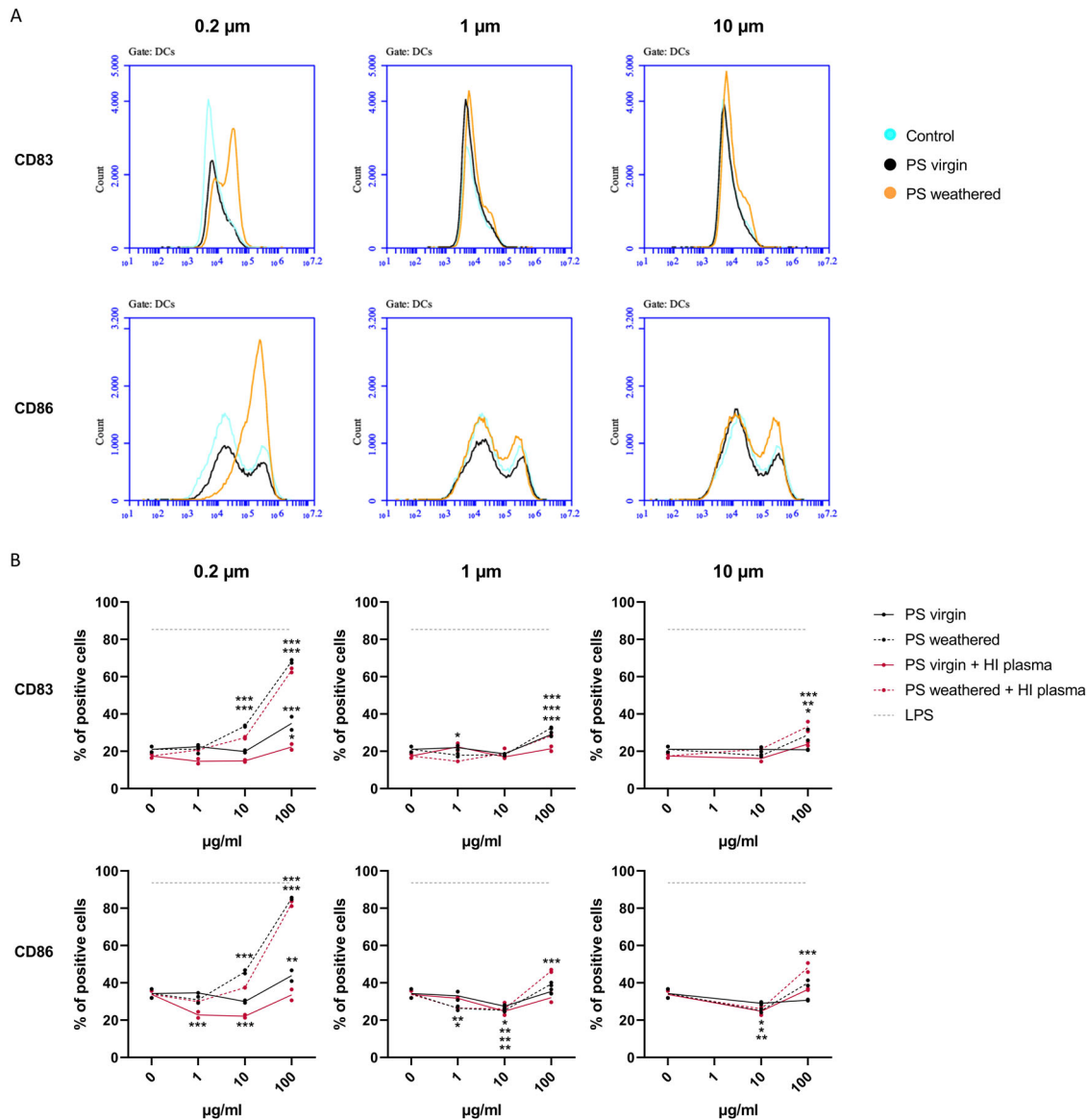


Figure 4. Weathered 0.2 µm PS particles activate human DC. Human (monocyte-derived) dendritic cells were exposed to LPS (500 ng/ml) or non-fluorescent virgin or weathered PS particles (1–100 µg/ml, pre-incubated for 1 h at 37 °C with PBS or heat-inactivated (HI) plasma) for 24 h. Expression of co-stimulatory markers CD83 and CD86 was measured by flow cytometry on live-gated cells. (A) Histograms are shown of the fluorescence intensity for the different exposure groups at 100 µg/ml. (B) CD83 and CD86 expression is presented by the percentage of positive cells. *** $p < 0.001$, ** $p < 0.01$, * $p < 0.05$ compared to control.

the MoDC. A clear increase in fluorescence intensity was visible for the 0.2 µm PS weathered particles, indicating up-regulation of CD83 and CD86. Figure 4(B) shows that the CD83 and CD86 up-regulation caused by 0.2 µm PS weathered particles starts at a concentration of 10 µg/ml, regardless of HI plasma pre-incubation. The magnitude of the effect at 100 µg/ml of 0.2 µm PS weathered particles was comparable to that of the positive LPS control. Virgin 0.2 µm PS particles only caused a very minor increase of CD83 and CD86 at a concentration of 100 µg/ml. Also, 1 µm PS and 10 µm PS virgin particles, caused a minor increase in co-stimulatory markers, regardless of pre-incubation with HI plasma.

Notably, the number and surface area of 0.2 µm particles at the mass concentration of 10 µg/ml are much higher compared to the 1 and 10 µm particles (see Table 1). The number of 0.2 µm particles was ≈ 100 - or 100,000-fold higher, and the surface area was ≈ 10 - to 100-fold larger compared to the 1 and 10 µm particles, respectively.

Weathered PS particles increase dendritic cell-induced T-cell proliferation in MLR assay

To test MoDC for their ability to stimulate T-cells, allogeneic T-cells were added to a MLR assay. Figure 5(A) shows the division of the CD8 T-cells that were stimulated with weathered 0.2 and 1 and 10 µm PS particle-exposed MoDC. As observed in these histograms, dilution of cell tracer violet in CD8 T-cells was particularly visible for the weathered 0.2 and 1 µm PS particles. The division index was calculated, indicating the average number of cell divisions of one cell in the original population. The results show that MoDC significantly induced CD8 T-cell division when exposed to weathered 0.2 µm PS particles compared to control and virgin 0.2 µm PS particles (Figure 5(B)). These findings confirm that after exposure to weathered 0.2 µm PS particles, MoDC expressed the necessary signals to stimulate CD8 T-cells in a non-antigen-driven manner. There was no significant increase in the proliferation of CD4 cells.

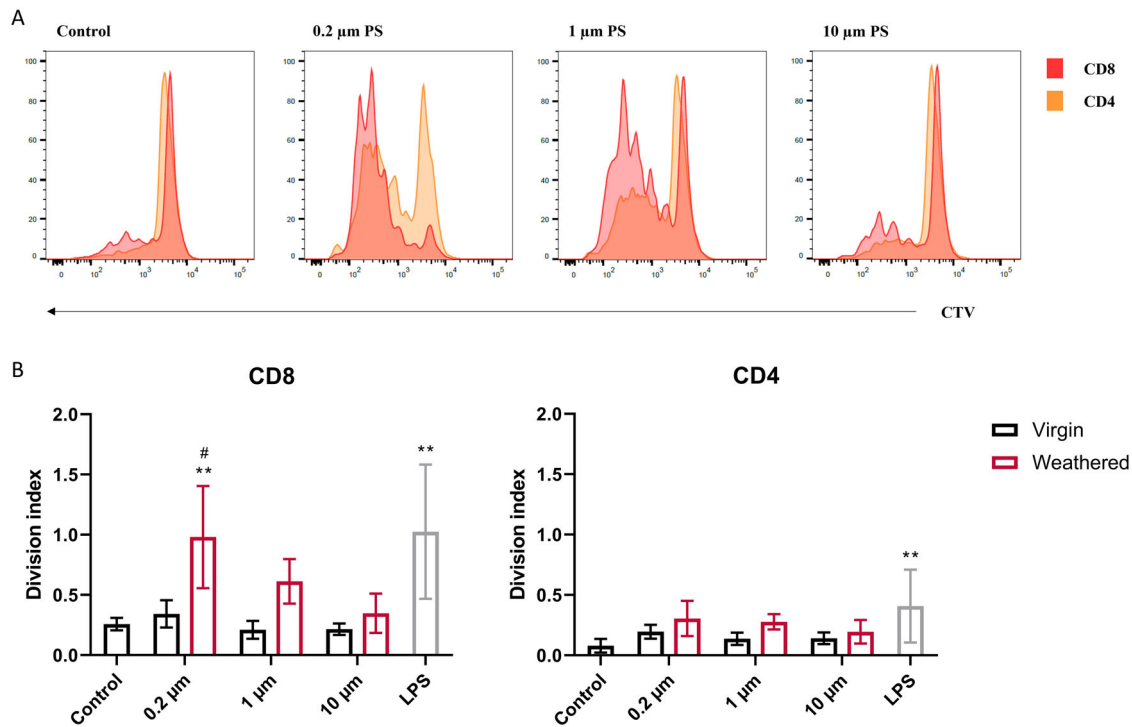


Figure 5. Weathered 0.2 μm PS particles increase T-cell division without extra maturation. Human (monocyte-derived) dendritic cells were exposed to 0.2, 1, or 10 μm virgin and weathered PS particles (100 $\mu\text{g}/\text{ml}$, pre-incubated for 1 h at 37 $^{\circ}\text{C}$ with heat-inactivated plasma [HI plasma]). A mixed leukocyte reaction (MLR) assay was performed by adding T-cells from a different donor to the cell culture. (A) Histograms of dilution of Cell tracer violet (CTV) of CD8 and CD4 T-cells stimulated with MoDC exposed to weathered PS particles. (B) The average of either CD8 or CD4 T-cells that went into division after stimulation with PS particle-loaded DC from another donor. Data are presented as means \pm SD. *** $p < 0.001$, ** $p < 0.01$, * $p < 0.05$ compared to control. ### $p < 0.01$, ## $p < 0.01$, # $p < 0.05$ compared to virgin PS.

Discussion

This study aimed to provide detailed *in vitro* information regarding the uptake and the potential immunotoxic effect of virgin and weathered MNP in human MoDC. Overall, the findings here suggest that DC take up PS particles up to 10 μm . Depending on their size, weathered PS particles induced a more profound phenotypical and functional maturation of DC than virgin PS particles. The present data show that, in particular, weathered small-sized (0.2 μm) MNP stimulate DC to express co-stimulatory molecules (i.e. CD83 and CD86) and to elicit (allogeneic) T-cell activation.

In this study, flow cytometry and imaging show that pristine 0.2 and 1 μm PS particles are readily taken up by MoDC after 1 h of incubation time. Such uptake is in line with previous research showing that MoDC take up PS particles with diameters ranging from 0.078 to 4.5 μm (Foged et al. 2005; Rothen-Rutishauser et al. 2007; Weber et al. 2022). Moreover, as confirmed here, previous studies have shown that the interaction of MNP with immune cells is size-dependent (Foged et al. 2005; Seydoux et al. 2014; Mathaes et al. 2015). This study confirmed that with decreasing particle size, the percentage of DC interacting with the PS particles increased. STORM images also showed that smaller PS particles occupy less volume, which allows more particles to be contained within one cell. An explanation for this size-dependent interaction might be that different uptake mechanisms are involved for the different sizes of PS particles. Notably, Baranov et al. (2021) reviewed and modeled the uptake and processing capacities of immune cells based on several types of model particles with a wide diversity in shape, size, rigidity, and surface roughness. They found that particles smaller than 0.5 μm were taken up via endocytosis, whereas particles bigger than

0.5 μm were taken up via phagocytosis. Nevertheless, the extent to which these mechanisms influence MNP uptake in DC is still unknown, and further studies are needed to investigate the kinetics of MNP.

PS particles injected intravenously are rapidly covered by blood proteins and the resulting protein biofilm has been shown to play an important role in particle-cell interaction, favoring their uptake (Lesniak et al. 2010; Tenzer et al. 2013; Schöttler et al. 2016). However, the influence of the blood-derived biofilm on MNP uptake by DC is still not well-investigated. The study here showed that pre-incubating the particles in HI human plasma significantly enhanced 0.2 μm PS particle uptake by MoDC. The uptake of 1 μm PS particles was reduced, whereas the uptake of 10 μm PS particles was only observed when the particles were pre-incubated in HI plasma. Heat-labile components of human plasma such as serum complement are not likely to be involved in the uptake observed in this study, as they were inactivated by heat-inactivation of the plasma. However, blood contains dozens of other proteins that can act as opsonins, facilitating uptake by phagocytes (Walkey et al. 2012). This highlights that the protein biofilm cannot be neglected when researching the uptake of MNP.

DC maturation – needed as a first step in the induction of antigen-specific T-cell activation – is characterized by the up-regulation of co-stimulatory cell surface markers such as CD83 and CD86 (Frick et al. 2012; Al-Ashmawy 2018). This study showed that weathered 0.2 μm PS particles could increase the expression of CD83 and CD86 on the surface of DC cells in a dose-dependent manner, starting at 10 $\mu\text{g}/\text{ml}$. It has been suggested that nano-sized particles, such as gold particles, can be more reactive than micro-sized particles due to their larger

surface area (Shin et al. 2015). According to the present results, one can conclude that this principle also seems to apply to PS particles. As indicated, a fixed mass of smaller particles has a higher amount and larger total surface area compared to the same mass of larger particles (Table 1). This may add to the findings that smaller particles induce higher expression of the co-stimulatory markers.

The study here also showed that weathered PS particles were significantly more effective in inducing CD83 and CD86 expression than virgin particles. This could suggest the involvement of additional chemical or microbial components such as endotoxins present in the biofilm of weathered particles. Notably, chemical profiling of the pristine and weathered PS particles used in this study revealed that the weathering process causes a change in the chemical composition of the PS particle (Dusza et al. 2022).

In contrast to what has been seen with regard to PS particle uptake, pre-incubation of particles in HI plasma had very little effect on the activation of human MoDC. This finding might suggest that uptake of and cellular activation by weathered particles might not be directly correlated. Another explanation could be that, unlike as observed with the 10 µm PS particles, weathering might influence the uptake of smaller PS particles.

Importantly, this study showed with a MLR assay that DC exposed to weathered 0.2 µm PS particles could increase T-cell division. It has already been known for more than a decade that other particles (such as ultrafine carbon black) can induce phenotypical and functional maturation of DC and act as adjuvants (de Haar et al. 2008). The present results implicate that, like carbon black-treated DC, weathered NP-treated DC can exhibit an enhanced capacity to stimulate T-cell division. This indicates that weathered PS particles have immunostimulating adjuvant properties that might lead to an increased risk of immune sensitization.

Data on the effects of PS particles on DC-mediated T-cell activation are scarce. However, the available research agrees with the results that were found here, particularly concerning size and surface chemistry. For instance, Mathaes et al. (2015) showed that, compared to 2 µm PS particles, 150 nm PS particles pre-incubated with TLR ligands, are internalized more efficiently and cause increased expression of CD83 and CD86 on the surface of DC. Furthermore, Frick et al. (2012) investigated the immunomodulatory properties of PS NPs and, in line with the results here, it was seen that virgin particles did not enhance T-cell activation. However, those investigators found that sulfonate- and phosphonate-functionalized PS particles enhanced DC maturation, resulting in the increased capacity to stimulate T-cells. Other studies also showed that to enhance DC maturation, the surface of the MNP needs modification, for instance by loading the surface with specific antibodies or ligands (Kempf et al. 2003; Mathaes et al. 2015). This, together with the current findings that weathered PS particles were more reactive than virgin particles, confirms that the surface chemistry of PS particles is an important factor influencing their immunotoxicity.

Despite best efforts, some common concerns and limitations in the emerging field of MNP research could not be avoided. The most important concern relates to dosimetry used during exposure. As no consensus exists regarding dose metrics, we chose to expose mass-based in this study as detection in human matrices is also described in mass concentrations (Leslie et al. 2022). However, the actual concentration of PS particles in contact with the DC is important but, unfortunately, still technically challenging to control due to unknown buoyancy, sedimentation, and aggregation rates over time. Optimized and standardized

exposure procedures are therefore required and essential for proper risk assessment regarding MNP.

Furthermore, MNP research is limited by the particles that are available and are still uniform in shape and composition. This study conducted experiments using commercially-available PS particles of uniform shape but different sizes. In addition, PS particles were used that had undergone a laboratory-controlled weathering process to simulate more environmentally relevant particles. However, humans are exposed to a heterogeneous mixture of MNP that vary in polymer type, size, shape, and biofilm. Therefore, for proper hazard assessment, the characterization of the effect of MNP with different physicochemical properties on DCs is important.

In conclusion, this study aimed to investigate the effect of virgin and weathered MNP on the functional maturation of human monocyte-derived DC. The findings shown here suggest that nano-sized weathered MNP modulate the immune system, acting through the initiation of phenotypic and functional maturation of DC. Furthermore, particle-cell interaction may be underestimated in the absence of environmental aging. Therefore, MNP cannot be studied as a homogeneous substance and it is, therefore, essential to consider particle size, surface, and biofilm characteristics when assessing the immunotoxicity of MNP as a whole.

Acknowledgments

Ig. Rianne van den Meiracker and Dr. Bas van der Zaan (Deltares, the Netherlands) are acknowledged for providing the virgin and weathered PS particles. The authors also thank Ing. Esther van t Veld and Dr. Richard Wubolts for their help and expertise during the imaging. Furthermore, the authors thank Dr. Nienke Vrisekoop and Joëlle Klazen (UMC Utrecht, the Netherlands) for their help with the in-house donor service.

Disclosure statement

No potential conflict of interest was reported by the author(s). The authors alone are responsible for the content of this manuscript.

Funding

This study was supported by the Netherlands Organization for Health Research and Development (ZonMw) under the Microplastic and Health Programme [Grant #458001009, 40-45800-98-112], led by Dr. J.J. Smit. Currently, A.E.T. van den Berg is appointed within the framework of EC Horizon 2020-project POLYRISK [Grant ID 964766], led by Dr. R.H.H. Pieters. Dr. J. Legler, Dr. D. Vethaak, Dr. R.H.H. Pieters and K.J. Adriaans are also involved in the ZonMw/Health Holland project MOMENTUM [Grant ID 458001101].


ORCID

Annemijne E. T. van den Berg  <http://orcid.org/0000-0001-7629-7750>

Maud Plantinga  <http://orcid.org/0000-0002-2328-3184>

Dick Vethaak  <http://orcid.org/0000-0001-9717-0919>

Kas J. Adriaans  <http://orcid.org/0000-0003-4474-3052>

Marianne Bol-Schoenmakers  <http://orcid.org/0000-0002-5917-4406>

Juliette Legler  <http://orcid.org/0000-0001-6321-1567>

Joost J. Smit  <http://orcid.org/0000-0003-4612-4036>
 Raymond H. H. Pieters  <http://orcid.org/0000-0002-3427-8401>

References

- Al-Ashmary G. 2018. Dendritic cell subsets, maturation and function. Dendritic cells. London: IntechOpen; p. 11–24.
- Andrady A. 2017. The plastic in microplastics: A review. Mar Pollut Bull. 119(1):12–22.
- Baranov M, Kumar M, Sacanna S, Thutupalli S, van den Bogaart G. 2021. Modulation of immune responses by particle size and shape. Front Immunol. 2021:3854.
- Barboza L, Vethaak A, Lavorante B, Lundebye A, Guilhermino L. 2018. Marine microplastic debris: An emerging issue for food security, food safety and human health. Mar Pollut Bull. 133:336–348.
- Boyles MSP, Kristl T, Andosch A, Zimmermann M, Tran N, Casals E, Himly M, Puentes V, Huber CG, Lütz-Meindl U, et al. 2015. Chitosan functionalization of gold nanoparticles encourages particle uptake and induces cytotoxicity and pro-inflammatory conditions in phagocytic cells, as well as enhancing particle interactions with serum components. J Nanobiotechnol. 13(1):1–20.
- Carbery M, O'Connor W, Palanisami T. 2018. Trophic transfer of microplastics and mixed contaminants in the marine food web and implications for human health. Environ Int. 115:400–409.
- Coombes J, Powrie F. 2008. Dendritic cells in intestinal immune regulation. Nat Rev Immunol. 8(6):435–446.
- Cox K, Covernton G, Davies H, Dower J, Juanes F, Dudas S. 2019. Human consumption of microplastics. Environ Sci Technol. 53(12):7068–7074.
- de Haar C, Kool M, Hassing I, Bol M, Lambrecht B, Pieters R. 2008. Lung dendritic cells are stimulated by ultrafine particles and play a key role in particle adjuvant activity. J Allergy Clin Immunol. 121(5):1246–1254.
- Dusza H, Katrukha E, Nijmeijer S, Vethaak A, Walker D, Legler J. 2022. Uptake, transport and toxicity of pristine and weathered micro- and nano-plastics in human placenta cells. Environ Health Perspect. 130:97006.
- [EFSA] European Food Safety Authority. 2016. Presence of microplastics and nanoplastics in food, with particular focus on seafood. EFSA J. 14:e04501.
- Foged C, Brodin B, Frokjaer S, Sundblad A. 2005. Particle size and surface charge affect particle uptake by human dendritic cells in an *in vitro* model. Int J Pharm. 298(2):315–322.
- Frick S, Bacher N, Baier G, Mailänder V, Landfester K, Steinbrink K. 2012. Functionalized polystyrene nanoparticles trigger human dendritic cell maturation resulting in enhanced CD4⁺ T-cell activation. Macromol Biosci. 12(12):1637–1647.
- Gruber MM, Hirschmugl B, Berger N, Holter M, Radulović S, Leitinger G, Liesinger L, Berghold A, Roblegg E, Birner-Gruenberger R, et al. 2020. Plasma proteins facilitates placental transfer of polystyrene particles. J Nanobiotechnol. 18(1):14.
- Hidalgo-Ruz V, Gutow L, Thompson R, Thiel M. 2012. Microplastics in the marine environment: A review of the methods used for identification and quantification. Environ Sci Technol. 46(6):3060–3075.
- Hirt N, Body-Malapel M. 2020. Immunotoxicity and intestinal effects of nano- and microplastics: A review of the literature. Part Fibre Toxicol. 17(1):1–22.
- Ke P, Lin S, Parak W, Davis T, Caruso F. 2017. A decade of the protein corona. ACS Nano. 11(12):11773–11776.
- Kempf M, Mandal B, Jilek S, Thiele L, Vörös J, Textor M, Merkle H, Walter E. 2003. Improved stimulation of human dendritic cells by receptor engagement with surface-modified micro-particles. J Drug Target. 11(1):11–18.
- Koelmans A, Besseling E, Foekema E, Kooi M, Mintenig S, Ossendorp B, Redondo-Hasseler-Harm P, Verschoor A, van Wezel A, Scheffer M. 2017. Risks of plastic debris: Unravelling fact, opinion, perception, and belief. Environ Sci Technol. 51(20):11513–11519.
- Leslie H, van Velzen M, Brandsma S, Vethaak A, Garcia-Vallejo J, Lamoree M. 2022. Discovery and quantification of plastic particle pollution in human blood. Environ Int. 163:107199.
- Lesniak A, Campbell A, Monopoli M, Lynch I, Salvati A, Dawson K. 2010. Serum heat inactivation affects protein corona composition and nanoparticle uptake. Biomaterials. 31(36):9511–9518.
- Li Y, Shi Z, Radauer-Preiml I, Andosch A, Casals E, Luetz-Meindl U, Cobaleda M, Lin Z, Jaber-Douraki M, Italiani P, et al. 2017. Bacterial endotoxin (lipopolysaccharide) binds to the surface of gold nanoparticles, interferes with biocorona formation and induces human mono-cyte inflammatory activation. Nanotoxicology. 11(9–10):1157–1175.
- Mathaes R, Winter G, Siahaan T, Besheer A, Engert J. 2015. Influence of particle size, an elongated particle geometry, and adjuvants on dendritic cell activation. Eur J Pharm Biopharm. 94:542–549.
- Noventa S, Boyles M, Seifert A, Belluco S, Jiménez A, Johnston H, Tran L, Fernandes T, Mughini-Gras L, Orsini M. 2021. Paradigms to assess the human health risks of nano- and microplastics. Microplast Nanoplast. 1: 1–27.
- Prata J, da Costa J, Lopes I, Duarte A, Rocha-Santos T. 2020. Environmental exposure to micro-plastics: An overview on possible human health effects. Sci Total Environ. 702:134455.
- Rothen-Rutishauser B, Mühlfeld C, Blank F, Musso C, Gehr P. 2007. Translocation of particles and inflammatory responses after exposure to fine particles and nanoparticles in an epithelial airway model. Part Fibre Toxicol. 4:9–9.
- [SAPEA] Science Advice for Policy by European Academies. 2019. A scientific perspective on microplastics in nature and society. Berlin, Germany: SAPEA.
- Saptarshi S, Duschl A, Lopata A. 2013. Interaction of nanoparticles with proteins: Relation to bio-reactivity of the nanoparticle. J Nanobiotechnol. 11(1):1–12.
- Schöttler S, Klein K, Landfester K, Mailänder V. 2016. Protein source and choice of anticoagulant decisively affect nanoparticle protein corona and cellular uptake. Nanoscale. 8(10):5526–5536.
- Senathirajah K, Attwood S, Bhagwat G, Carbery M, Wilson S, Palanisami T. 2021. Estimation of the mass of microplastics ingested: A pivotal first step towards human health risk assessment. J Hazard Mater. 404(Pt B):124004.
- Seydoux E, Rothen-Rutishauser B, Nita I, Balog S, Gazdhar A, Stumbles P, Petri-Fink A, Blank F, Von Garnier C. 2014. Size-dependent accumulation of particles in lysosomes modulates dendritic cell function through impaired antigen degradation. Int J Nanomedicine. 9:3885–3902.
- Shin S, Song I, Um S. 2015. Role of physicochemical properties in nanoparticle toxicity. Nanomaterials (Basel). 5(3):1351–1365.
- Stagg A. 2018. Intestinal dendritic cells in health and gut inflammation. Front Immunol. 2018:2883.
- Tenzen S, Docter D, Kuharev J, Musyanovych A, Fetz V, Hecht R, Schlenk F, Fischer D, Kiouptsi K, Reinhardt C, et al. 2013. Rapid formation of plasma protein corona critically affects nanoparticle pathophysiology. Nat Nanotechnol. 8(10):772–781.
- Tourkova I, Yurkovetsky Z, Shurin M, Shurin G. 2001. Mechanisms of dendritic cell-induced T-cell proliferation in the primary MLR assay. Immunol Lett. 78(2):75–82.
- Vethaak A, Legler J. 2021. Microplastics and human health: Knowledge gaps should be addressed to ascertain the health risks of microplastics. Science. 371(6530):672–674.
- Walkey C, Olsen J, Guo H, Emili A, Chan W. 2012. Nanoparticle size and surface chemistry determine serum protein adsorption and macrophage uptake. J Am Chem Soc. 134(4):2139–2147.
- Weber A, Schwiebs A, Solhaug H, Stenvik J, Nilsen AM, Wagner M, Relja B, Radeke H. 2022. Nanoplastics affect the inflammatory cytokine release by primary human monocytes and dendritic cells. Environ Intl. 163:107173.
- [WHO] World Health Organization. 2022. Dietary and inhalation exposure to nano- and microplastic particles and potential implications for human health. Geneva, Switzerland: World Health Organization. Licence: CC BY-NC-SA 3.0 IGO.
- Witzmann T, Ramsperger A, Wieland S, Laforsch C, Kress H, Fery A, Auernhammer G. 2022. Repulsive interactions of eco-corona-covered microplastic particles quantitatively follow modeling of polymer brushes. Langmuir. 38(29):8748–8756.